Prediction of Mechanical Performance of Acetylated MDF at Different Humid Conditions

Sheikh Ali Ahmed [1],* , Stergios Adamopoulos [2],* , Junqiu Li [1] and Janka Kovacikova [3]

[1] Department of Forestry and Wood Technology, Faculty of Technology, Linnaeus University, Georg Lückligs Plats 1, 351 95 Växjö, Sweden; jl223hc@student.lnu.se

[2] Department of Forest Biomaterials and Technology, Division of Wood Science and Technology, Vallvägen 9C-D, 756 51 Uppsala, Sweden

[3] Department of Mechanical Engineering, Faculty of Technology, Linnaeus University, Georg Lückligs Plats 1, 351 95 Växjö, Sweden; janka.kovacikova@lnu.se

* Correspondence: sheikh.ahmed@lnu.se (S.A.A.); stergios.adamopoulos@slu.se (S.A.); Tel.: +46-470-76-7492 (S.A.A.); +46-018-67-2474 (S.A.)

Abstract: Change of relative humidity (RH) in surrounding environment can greatly affect the physical and mechanical properties of wood-based panels. Commercially produced acetylated medium density fiberboard (MDF), Medite Tricoya®, was used in this study to predict strength and stiffness under varying humid conditions by separating samples in parallel (//) and perpendicular ($\perp$) to the sanding directions. Thickness swelling, static moduli of elasticity (MOE_{stat}) and rupture (MOR_{stat}), and internal bond (IB) strength were measured at three different humid conditions, i.e., dry (35% RH), standard (65% RH) and wet (85% RH). Internal bond (IB) strength was also measured after accelerated aging test. A resonance method was used to determine dynamic modulus of elasticity (MOE_{dyn}) at the aforementioned humid conditions. Linear regression and finite element (FE) analyses were used to predict the MDF's static bending behavior. Results showed that dimensional stability, MOE_{stat}, MOR_{stat} and IB strength decreased significantly with an increase in RH. No reduction of IB strength was observed after 426 h of accelerated aging test. A multiple regression model was established using MOE_{dyn} and RH values to predict MOE_{stat} and MOR_{stat}. In both directions (// and $\perp$), highly significant relationships were observed. The predicted and the measured values of MOE_{stat} and MOR_{stat} were satisfactorily related to each other, which indicated that the developed model can be effectively used for evaluating the strength and stiffness of Medite Tricoya® MDF samples at any humid condition. Percent errors of two different simulation techniques (standard and extended FE method) showed highly efficient way of simulating the MDF structures with low fidelity.

Keywords: acetylation; wood fiber; strength; stiffness; internal bonding strength; thickness swelling; regression; finite element analysis

1. Introduction

Medium density fiberboard (MDF) is manufactured with wood fibers bonded with water resistant adhesives such as phenol formaldehyde, urea formaldehyde, isocyanate resin, etc. [1,2]. MDF is primarily used in furniture, as a building material and for laminate flooring, since it has good strength and stiffness and it is easy to process. Compared to plywood, MDF panels generally swell more and may not be recovered after drying due to the inherent hygroscopicity of the wood fibers, the residual stresses formed in the fiber mat during hot pressing and some loss of the glue bonds [3]. As a result, when the MDF panel is exposed to any form of water, its constituent wood fibers swell and some of that residual stress is released, resulting in an increase of thickness of the panel. Thickness swelling

markedly weakens the product [4], and the mechanical properties that are most directly affected are shear strength and moduli of elasticity and rupture [5]. Exposure to outdoor environment with varying climate conditions can result in dimensional changes and strength loss, and thus MDF panels are generally not recommended for exterior applications. In terms of computational modelling, these phenomena are considered to be the rheological behavior of the material [6].

Several studies have been carried out using various adhesive systems [7–9], post treatments [10], heat treated fibers [11], alternative fibers [12] and recycled adhesives [13] to improve strength and water resistance of MDF panels. In addition, chemical modification was also used to improve the material properties, such as moisture-related properties, durability and weathering resistance [14–16]. The most described chemical modification method for improved dimensional stability of wood particles and fibers to produce panel products is acetylation with acetic anhydride [17,18]. In acetylation process, acetic anhydride substitutes the hydroxyl (-OH) groups in the wood cells with acetyl groups, resulting in decreased hygroscopicity and increased dimensional stability; while reductions in some mechanical properties also occur depending on the extent of temperature and time of the modification reaction [18–20]. Several explanations of the strength loss were given, as for example the type of the adhesive [21], bondability [22], press pressure [23], etc. Higher bondability is required if the panels are used under severe conditions for a long time. Thus, the effect of weathering on the dimensional changes and mechanical properties of acetylated MDF would be beneficial for predicting its long-term service behavior. Mechanical strength and stiffness along and perpendicular to the sanding direction should be also available to achieve better and proper assembly of acetylated MDF panels in outdoor applications.

Fiberboards can be exposed to a range of environmental conditions during service life. Moisture content of MDF, similar to other lignocellulosic materials, changes with the change of surrounding humidity and temperature. Therefore, it is important to know the relationship between moisture content and strength properties of MDF if used as a structural member subjected to these environmental conditions. Use of non-destructive acoustic testing could provide a rapid and reliable measurement of strength properties of MDF panels. Usually, acoustic testing is carried out by using time-of-flight (TOF) and resonance methods [24]. TOF methods use propagation time of a pulse of ultrasound or a stress wave across the material. On the other hand, resonance methods use the free vibration frequency of the material under forced harmonic vibration. Resonance methods provide more information on the elastic properties of materials and are thus considered more reliable than the TOF methods [25]. Previous studies showed a very good to strong relation between dynamic bending properties measured by acoustic tools with the static bending properties of wood panels [26,27]. However, values of dynamic bending properties vary depending on the method used and, most importantly, on the moisture content levels of wood panels. Prediction of static bending properties of acetylated MDF using acoustic techniques under different humid conditions is lacking. Considering that acetylated MDF is more hydrophobic than conventional MDF, fewer internal bond failures and associated changes of internal structure should be expected by repeated swelling and shrinkage. That in turn should lead to more stable static bending behavior. Nevertheless, establishing the relationship between acoustic and static bending properties of acetylated MDF at different humid conditions would ensure reliable and safe predictions of their performance for intended end uses.

Another available method to predict and analyze material behavior of MDF is creating macro scale finite element (FE) models of MDF board's structure. Following classic design procedures for macroscale modelling, the material characteristics obtained from the experiments presented in this paper were used as input values to define the material, and the geometry and boundary conditions of the experiment set up were imitated in the FE model. Here, two analysis approaches that are implemented in a SIMULIA™ Abaqus/CEA (Systèmes®) were used to imitate a static three-point bending test. The first approach was a standard quasi-static stress/displacement procedure to control the time incrementation, and the approach is named T1 in this work [28]. Additionally, a second and more advanced technique, the extended finite element method (XFEM) [29], was used and is named T2. This technique allows us to model discontinuities as an enriched feature and it is an extension to

the conventional finite element method [28]. Both techniques are classified as macroscale techniques that are nowadays typically used while designing structures [30,31]. The outcome of both analyses are displacements, reaction forces and maximum principal stresses of the studied FE models. These models should be later optimized to achieve higher fidelity, meaning to create more sophisticated models accounting for the environmental loads as well as mechanical loads, for example, multiscale models [32].

Yet, there is not enough systematic information on the dimensional stability and mechanical properties of acetylated MDF panels under different humid conditions. Establishing correlations between elastic properties measured nondestructively with bending strength and stiffness of acetylated MDF would lead to a quick and reliable means of assessment of the safety margins for different applications. Thus, this study was focused on elucidating the dimensional and static bending properties of acetylated MDF and on evaluating possibilities to predict its bending behavior from acoustic data by using standard statistical and multiscale prediction modelling methods. Dry (35% RH), standard (65% RH) and wet (85% RH) climatic conditions were considered to represent different moisture content situations as well as accelerated weathering.

2. Materials and Methods

2.1. MDF Panels

Commercially produced Medite Tricoya® MDF panels with dimensions of $300 \times 210 \times 18$ mm^3 (length × width × thickness) were used in this study. Formaldehyde free glue is used for the acetylated softwood fibres during the production of Tricoya ® panels. Two different sample sets were prepared, i.e., along (parallel samples symbolized by //) and across (perpendicular samples symbolized by ⊥) the sanding direction. Working samples were prepared according to Table 1 and were stored in three different climatic conditions, i.e., dry (20 °C, 35% RH), standard (20 °C, 65% RH) and wet (20 °C, 85% RH). Five replicates of MDF samples (two different directions and three climatic conditions depending on measured properties) were produced in a total of 80 samples, which were tested for different properties according to EN standards (Table 1).

Table 1. Dimensions (length × width × thickness) of samples used for measuring different physical and mechanical properties of Medite Tricoya® medium density fiberboard (MDF) samples.

Type	Properties Measured	Dimensions [mm^3]	Sample Number	Standard Followed
Physical properties	Moisture content	$50 \times 50 \times 18$	15	EN 322 [33]
	Density	$50 \times 50 \times 18$	15	EN 323 [34]
	Dimensional changes	$300 \times 50 \times 18$	10	EN 318 [35]
	Thickness swelling	$50 \times 50 \times 18$	5	EN 317 [36]
	Accelerated aging	$300 \times 70 \times 18$	5	
Mechanical properties	Internal bonding	$50 \times 50 \times 18$	15	EN 319 [37]
	Three-point bending	$300 \times 36 \times 18$	15	EN 310 [38]

Moisture content and density were measured on samples after conditioning in each climatic condition. Samples were considered to be acclimatized when the differences were smaller than the 0.1% mass of the sample between two weightings within 24 h.

2.2. Experimental

2.2.1. Dimensional Changes

The relative changes in length and thickness of the samples were determined in between two equilibrium conditions. The increases in length and thickness due to swelling were measured from 65% to 85% RH in adsorption (first regime), while the reductions in length and thickness due to shrinkage

were measured from 65% to 35% RH in desorption (second regime), according to the standard EN 318 [35]. The samples were exposed to different RH levels until acclimatized at two regimes. The first regime consisted of dimensional changes among consecutive RHs 35%, 65% and 85% at 20 °C constant temperature, whilst the second regime consisted of consecutive RHs in the reverse order, i.e., 85%, 65% and 35%, at 20 °C constant temperature.

Relative expansion and contraction sample's length were calculated using the formulae below:

$$\delta l_{65,85} \text{ (mm/m)} = 1000 \times (l_{85} - l_{65})/l_{65} \tag{1}$$

$$\delta l_{65,35} \text{ (mm/m)} = 1000 \times (l_{35} - l_{65})/l_{65} \tag{2}$$

where $\delta l_{65,85}$ (mm/m) is the relative increase in length due to swelling of sample's length after RH change from 65% to 85%, based on the length l (mm) measured at 65% RH and 85% RH; $\delta l_{65,35}$ (mm/m) is the relative reduction in thickness due to the shrinkage sample's length after RH change from 65% to 35%, based on the length l (mm) measured at 65% RH and 35% RH.

Similar to the calculations of relative change in the sample's length, thickness swelling and shrinkage properties were calculated as follows:

$$\delta t_{65,85} \text{ (\%)} = 100 \times (t_{85} - t_{65})/t_{65} \tag{3}$$

$$\delta t_{65,35} \text{ (\%)} = 100 \times (t_{35} - t_{65})/t_{65} \tag{4}$$

where $\delta t_{65,85}$ (%) is the relative increase in sample´s thickness due to swelling after RH change from 65% to 85%, based on the thickness t (mm) measured at 65% RH and 85% RH; $\delta t_{65,35}$ (%) is the reduction of the sample's thickness due to shrinkage after RH change from 65% to 35%, based on the thickness t (mm) measured at 65% RH and 35% RH.

2.2.2. Thickness Swelling

In this test, conditioned samples at 20 °C and 65% RH were placed in swelling testers (IMAL SW 200, San Damaso, Italy) having water pH of 7 ± 1, and the temperature was controlled to 20 ± 1 °C. Samples were immersed about 25 mm in water and were separated from each other and from the sides of the water bath. After immersion in water for 24 h, the thickness of each test piece was measured by a digital caliper nearest to 0.01 mm. Thickness swelling, G_t (%), was calculated based on the initial thickness t_1 (mm) before and final thickness t_2 (mm) after soaking in water.

$$G_t = 100 \times (t_2 - t_1)/t_1 \tag{5}$$

2.2.3. Accelerated Aging Test

All the edges of the samples were coated with silicone resin, conditioned at 20 °C and 65% RH and were placed in an QUV Accelerated Weathering Tester, QUV/spray (Q-Lab Co., Westlake, NJ, USA). This QUV with AUTOCAL system facilitates testing the external performance of products on their weather ability, light stability or corrosion resistance by simulating sunlight, rain and dew. The test was continued for 426 h and each complete cycle was equal to one week (168 h) following the sequence of condensation at 45 °C for under 24 h, a repeat of UV-radiation 60 °C (0.89 W/m^2/nm) at a wavelength of 340 nm for under 2.5 h and water spray (6–7 L/min) for under 0.5 h. One complete cycle was equal to one week (168 h). Commercial MDF of similar thickness (18 mm) intended for indoor use was used for comparison.

2.2.4. Non-Destructive Testing

An acoustic resonance method was used for measuring the dynamic modulus of elasticity (MOE$_{dyn}$). In this method, a data acquisition logger (PicoScope 4224, Cambridgeshire, UK) connected with the software BING®, version 9.7.2 (Beam Identification by Non-destructive Grading by CIRAD-

French Agricultural Research Centre for International Development, Montpellier, France) that controls, processes data and delivers results. A free-free flexural vibration test set-up was used, and more details about this method can be found in [39]. In flexural vibration, the first four modes of vibration were measured and used for determining the dynamic transversal modulus of elasticity, which represents stiffness under bending stress, i.e., MOE_{dyn}. The test was repeated four times for every sample, two times in each side, and the average was calculated.

2.2.5. Static Bending Test

A three-point bending test was performed to determine the static modulus of elasticity (MOE_{stat}) and modulus of rupture (MOR_{stat}) of the MDF samples following the standard EN 310 [38]. A universal testing machine (Instron 4466, Buckinghamshire, UK) with 10 kN load capacity was used. A static bending test was performed on the same sample used for measuring MOE_{dyn} in nondestructive testing. Uniaxial load was applied on the flat side of the samples. The load was constant (10 mm/m) so that the maximum load was reached within 60 ± 30 s. An increment of load and deflection between 10% and 40% of maximum load was considered for measuring the MOE_{stat} (MPa).

$$MOE_{stat} \ (MPa) = \{l^3(F_2 - F_1)\}/\{4bt^3(a_2 - a_1)\} \tag{6}$$

where l is the span length (mm), b is the width of sample (mm), t is the thickness of sample (mm), F_1 and F_2 are the increment of load at 10% and 40% of maximum load, and a_1 and a_2 are the corresponding deflection at the mid-length of the test pieces due to the load F_1 and F_2, respectively.

Bending strength, MOR_{stat} (MPa), of the test sample was calculated from the maximum load, F_{max} (N), using the equation:

$$MOR_{stat} \ (MPa) = (3F_{max}l)/(2bt^2) \tag{7}$$

2.2.6. Internal Bond Test

Internal bond (IB) or tensile strength perpendicular to the plane of panels was measured following the standard EN 319 [37]. Samples were effectively bonded with a hot-melt glue, and tensile load was applied until rupture using an Instron 4466 universal testing machine (Buckinghamshire, England) with 10 kN load capacity. A loading speed of 8 mm/min was maintained so that the maximum load is reached within 60 ± 30 s. In addition to the conditioned samples at dry (20 °C, 35% RH), standard (20 °C, 65% RH) and wet (20 °C, 85% RH) conditions, IB strength was also measured on samples after accelerated aging. IB or tensile strength (MPa) perpendicular to the plane of MDF test pieces was calculated by following the formula:

$$IB \ strength \ (MPa) = F_{max}/(ab) \tag{8}$$

where F_{max} is the breaking load (N), and a and b are the width (mm) and length (mm) of the test pieces, respectively.

2.2.7. Finite Element Analysis

Geometries of finite element (FE) models were identical to the samples manufactured for three-point bending tests and solved as a 3D problem; thus, full models were considered. Specifically, the beam´s part was 300 mm in length, 36 mm in width with a thickness of 18 mm, and the cylindrical pins' parts were 36 mm long with a diameter of 30 mm and placed 26 mm from both ends on a lower side of the beam part and in the middle of the beam´s span on an upper side of the beam part. The beam part was created as a deformable body and pins as discrete rigid bodies. The boundary conditions (BCs) and load were applied to the reference points (RP) created on pins' circular areas. Six degrees of freedom (df) were fixed in both bottom pins´ reference points for applying BCs and five df were set on the upper pin RP that also serves for applying a load. Namely, the following BCs were assigned: all six df are

fastened, thus 1, 2, 3, 4, 5, 6 = 0 for pins at the ends on the lower side of the beam part; for the pin in the middle of the span on the upper side of the beam part movement in the *z*-axis direction was enabled, only five df are fastened allowing movement in direction 3, thus 1, 2, 4, 5, 6 = 0. The global coordinate system and df notations and plus directions are shown in Figure 1. The load applied to the beam was a concentrated nodal force of value 1200 N, thus, larger than a mean value of the breaking load F_{max} measured in the experiment (Figure 1).
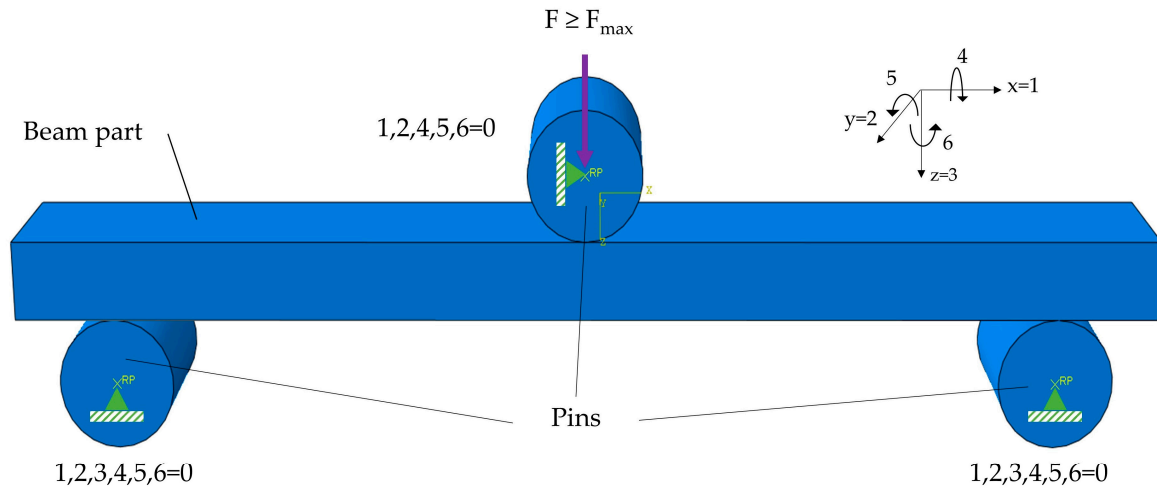

Figure 1. Illustration of parts and boundary conditions assigned in the finite element (FE) model.

3D rigid elements *R3D4* (4-node bilinear quadrilateral) and *R3D3* (3-node triangular facet) were assigned to mesh pins. To create a mesh for the beam, *C3D8R* (8-node linear brick) solid elements with reduced integration were defined.

Normal hard-contact, frictionless tangential behavior, and a general standard surface-to-surface contact, were prescribed to characterize the interaction between pin parts and the beam part. The mechanical properties of the elastic–plastic isotropic material of the studied MDFs had been taken from the experimental data considering the RH of 65% for the standard board perpendicular to bending: thus. Young´s modulus of 2574 MPa, Poisson´s ratio 0.25, and density of 746.2 kg/m^3.

Additionally, to specify a damage initiation, damage criteria for the XFEM model were prescribed to define the constitutive response for cohesive elements: namely, the maximum principal stress damage criterion (MAXPS) of value 34.47 MPa, taken from experiment measures. This means the damage criterion is using traction separation laws and is established as:

$$f = \{\langle\sigma_{max}\rangle/\sigma^0{}_{max}\} \tag{9}$$

where $\sigma^0{}_{max}$ represents the maximum allowable principal stress, and the symbol $\langle\ \rangle$ represents the Macaulay bracket with the usual interpretation. The Macaulay brackets are here to represent that a purely compressive stress does not initiate damage; rather, damage is initiated when the maximum nominal stress ratio reaches a value of one (f = 1) [28]. Additionally, there was no initial crack assigned to the model. Instead, the XFEM crack domain was designated on the whole beam part. For describing a crack geometry and the crack´s growth motion in 3D space, two level sets for a crack is assumed. First set is the crack surface Φ while second, Ψ, is made so the intersection of two level sets that gives the crack front. The nodal value of the function Φ is the signed distance of the node from the crack face and of the function Ψ is the signed distance of the node from an almost-orthogonal surface passing through the crack front [28].

2.2.8. Statistical Analysis

To determine any statistically significant differences between // and ⊥ samples, mean values were compared by a two-tailed group t-test at 0.05 significance level. In addition, to define relationships between measured parameters (MOE_{stat} and MOR_{stat}, MOR_{stat} and IB), linear regression analyses were performed.

Prediction models for MOE_{stat} and MOR_{stat} by using MOE_{dyn} and RH as input variables were built from multiple regression analysis using the following equation:

$$MOE_{stat} \text{ or } MOR_{stat} \text{ (predicted)} = MOE_{dyn} \times b_{MOEdyn} + RH \times b_{RH} + C \tag{10}$$

where b is coefficient and C is the intercept.

All regressions (linear, multiple) were performed at 95% confidence level using the Microsoft Excel 365 program (Microsoft, Redmond, WA, USA). In addition, the ANOVA is used to check the adequacy of the regression model developed.

3. Results and Discussion

3.1. Physical Properties

Moisture content, density and thickness swelling of commercially produced Medite Tricoya® MDF samples at three different RH levels are presented in Table 2. As expected, the EMC and density of samples increased with an increase in RH levels. Medite Tricoya® samples had 48% lower equilibrium moisture content when compared with commercial indoor MDF samples of similar thickness (Li et al., unpublished data) at 85% RH. Similar results can be found in a previous work [17]. As the acetylation process is a single site reaction, which means that one acetyl group is attached to one hydroxyl group resulting in a reduction of moisture absorption sites in wood polymers [40], acetylated MDF panels have low EMC even at high humidity level. Only 7.1% thickness swelling (after soaking in water for 24 h) was observed, meaning that acetylated panels do not swell severely when they are exposed to the water. These results showed that acetylation plays a significant role in the thickness swelling of the Medite Tricoya® samples. However, the extent of the reduced thickness swelling of acetylated MDF depends on the weight percent gain levels by acetylation process [2].

Table 2. Physical properties of Medite Tricoya® MDF samples at different RH levels. Values in parenthesis are the standard deviations.

Properties	35% RH	65% RH	85% RH
EMC (%)	4.6 (0.14)	7.6 (0.14)	7.9 (0.12)
Density (kg/m^3)	729.2 (9.59)	739.6 (1.37)	742.3 (7.51)
Thickness swelling (%) *		7.1 (0.36)	

* Thickness swelling is measured after immersion in water for 24 h at 20 °C.

Concerning the results of dimensional changes, the acetylation caused the MDF panels to absorb little moisture during the conditioning and are thus dimensionally stable (Table 3). The linear expansion of sample length and thickness swelling values obtained in adsorption conditions (relative humidity change from 65% to 85%) were higher than those values obtained in desorption conditions (relative humidity change from 65% to 35%). The amount of water held by wood fibers at a given temperature and RH depends on the direction from which equilibrium is approached. The moisture adsorbed at high relative humidity exposure is not entirely released when re-drying by lowering the relative humidity levels, and this phenomenon was well observed for wood-based panels in other studies [41,42]. As a result, acetylation had a major effect on the dimensional stability of Medite Tricoya® samples. In addition, the density of panels can also adversely affect the dimensional stability [41]. Average linear expansion and retraction of Medite Tricoya® samples were, respectively, 23% and 57% lower than

those of standard samples (Li et al., unpublished data) and for thickness changes, those differences were 67% and 45% (comparison was done from Li et al., unpublished data). However, no significant differences of relative shrinkage or swelling in thickness and length were observed in the two principle directions (// and ⊥ direction of sanding). An exception was seen for the relative swelling in length when RH increased from 65% to 85% where swelling was significantly higher in perpendicular samples. However, the reason for that is not quite clear.

Table 3. Relative changes in thickness and length of Medite Tricoya® MDF sample at different relative humidity (RH) levels. Values in parenthesis are the standard deviations.

Properties	Direction	Relative Change	
		$\delta_{65,35}$	$\delta_{65,85}$
Thickness (%)	//	−1.12 (0.08)	1.44 (0.07)
	⊥	−1.17 (0.07)	1.36 (0.03)
t-value		−0.905 [NS]	−2.140 [NS]
Length (mm/m)	//	−0.34 (0.03)	0.58 (0.08)
	⊥	−0.44 (0.09)	0.68 (0.03)
t-value		−1.819 [NS]	3.624 *

//: parallel sample to the sanding direction; ⊥: perpendicular sample to the sanding direction; $\delta_{65,35}$: samples conditioned from 65% to 35% RH; $\delta_{65,85}$: samples conditioned from 65% to 85% RH. * Significant at the 0.05 level as determined by two-sample t-test. NS, non-significant.

3.2. Mechanical Properties

Table 4 shows MOE$_{stat}$, MOR$_{stat}$ and IB properties of parallel and perpendicular samples from Medite Tricoya® MDF conditioned at dry, standard and wet conditions. With the increase of RH from 35 to 65%, the average MOE$_{stat}$ and MOR$_{stat}$ reduction of Medite Tricoya® samples was 8% and 10%, respectively. When the RH was further raised from 65% to 85%, reduction of those properties was respectively 37% and 20%. Higher humidity environment had a detrimental effect on the MOE$_{stat}$ and MOR$_{stat}$ and IB strength values for both sample types.

Table 4. Static bending properties and internal bond (IB) strength of Medite Tricoya® MDF samples. Values in parentheses are the standard deviations.

Direction	Dry, 35% RH			Standard, 65% RH			Wet, 85% RH		
	IB Strength [MPa]	MOE$_{stat}$ [MPa]	MOR$_{stat}$ [MPa]	IB Strength [MPa]	MOE$_{stat}$ [MPa]	MOR$_{stat}$ [MPa]	IB Strength [MPa]	MOE$_{stat}$ [MPa]	MOR$_{stat}$ [MPa]
//	0.99 (±0.08)	2938 (±43.38)	38.64 (±0.65)	0.79 (±0.10)	2670 (±61.28)	33.95 (±0.81)	0.57 (±0.07)	1656 (±46.94)	26.80 (±0.97)
⊥		2759 (±66.47)	35.73 (±0.99)		2557 (±76.30)	33.25 (±0.49)		1628 (±46.40)	26.77 (±0.63)
t-value		4.516 *	4.906 *		2.306 *	1.460 [NS]		0.841 [NS]	0.044 [NS]

//: parallel sample to the sanding direction; ⊥: perpendicular sample to the sanding direction. * Significant at the 0.05 level as determine by two-sample T test. NS, non-significant.

Mechanical properties like MOE$_{stat}$ and MOR$_{stat}$ measure the elastic behavior and resistance to bending, respectively, and are important properties when MDF is placed under load. Aforementioned properties determine largely the applicability of MDF as a structural component in furniture or other constructions. Those properties also depend on the sample properties, i.e., sanding direction (parallel or perpendicular), density, moisture content and type of MDF [2,5,43]. Dimensional stability is a good indication of the acetylation effect. However, moisture content had a great influence on the strength properties of both types of MDF samples. Significant reductions in MOE$_{stat}$, MOR$_{stat}$ and IB strength values were observed with an increase in RH (Table 4). These findings are in agreement with the

results found in previous studies [2,43]. The decrease in such properties at increasing RH level can be attributed to the separation of fibers resulting from the thickness swell of the panel materials [44]. Differences in the static bending properties were also found between parallel and perpendicular samples, and especially at the dry condition these differences were statistically significant. In general, MOE_{stat} and MOR_{stat} values were higher in parallel samples compared to perpendicular samples (see Table 4). Lower bending strength and stiffness values of perpendicular samples in MDF and other wood-based panels have been reported previously [26].

Figure 2 shows the linear regressions that determine how well the MOR_{stat} are related with MOE_{stat} values in parallel and perpendicular samples at different humid conditions. Statistical analysis showed strong positive and significant relationships ($p < 0.05$) for both sample directions (parallel and perpendicular) at varying humidity levels. Strong correlation between bending strength and modulus of elasticity is known for wood-based panels [45]. When linear regression analyses were performed by separating humid condition, very poor and insignificant relationships were observed. In the parallel samples, the coefficients of determination (R^2) were 0.08 and 0.39 at 65% and 85% RH, respectively; whilst in the perpendicular samples, those values were, respectively, 0.20 and 0.25. However, in a dry condition (35% RH), significant relationships ($p < 0.05$) were observed, and R^2 values were 0.85 and 0.88 in parallel and perpendicular samples, respectively. Previous findings also showed higher correlation coefficients at lower moisture content levels for wood-based panels [46,47].
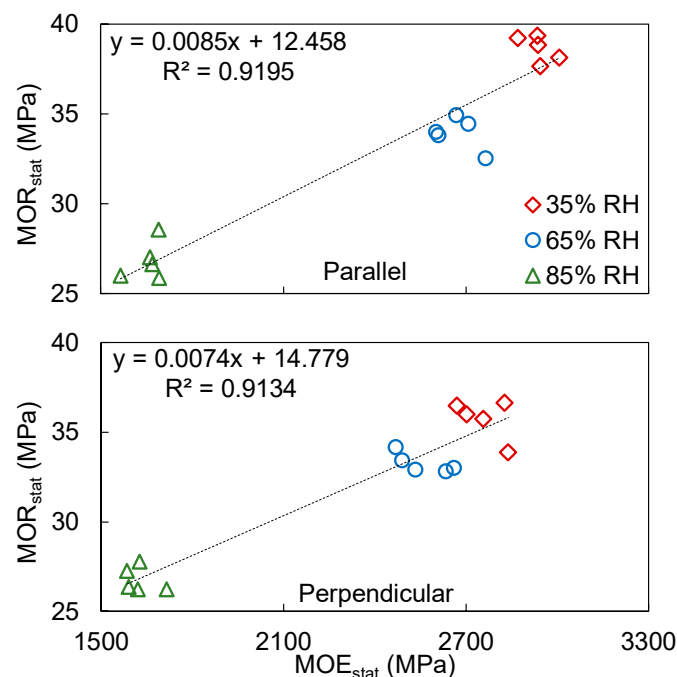

Figure 2. Linear relationship between MOE_{stat} and MOR_{stat} of the Medite Tricoya® medium density fiberboard (MDF) samples in two different directions conditioned at three different climatic conditions.

A positive and significant relationship ($p < 0.05$) between MOR_{stat} and IB was also observed (Figure 3). As shown in Table 4, Medite Tricoya® samples had the highest IB strength at 35% RH. With the increase of RH from 35 to 65%, the average IB strength reduction of Medite Tricoya® samples was 20%. When the RH was further raised from 65% to 85%, reduction of IB strength was 27%.

UV radiation causes photochemical degradation mainly in lignin polymers of the cell walls. UV light in combination with water plays a major role in such type of weathering. When lignin is degraded, water washes away degraded products and subsequently loosens the surface fibers to erode. However, acetylation reduces the loss of surface lignin and thus the erosion caused by accelerated weathering [48]. When compared with commercial MDF samples (indoor use), Medite Tricoya® samples performed much better in terms of the extent of being weathered by moisture and UV light. Thickness swelling

of the test pieces from indoor MDF was almost twice as much as Medite Tricoya® (Figure 4). After the accelerated aging test, fibers in the indoor samples were separated and were possible to shred by finger rub. That implied that no residual strength was left. Medite Tricoya® samples showed better resistance against thickness swelling. This could be attributed to the fiber–fiber bonding efficacy of the resin to retain bonding in a very hydrophobic fiber network. After accelerated aging and conditioning (20 °C, 65% RH), the IB strength of the Medite Tricoya® samples was found to be 0.79 ± 0.06 MPa. This result showed that Medite Tricoya® samples made from acetylated wood fibers were able to retain the initial IB strength of non-weathered samples. Previous results also showed that a higher residual strength was observed in acetylated MDF after a cyclic test [19]. Such retention of strength can also be attributed to other parameters than the acetylation of fibers, such as the adhesive used [49].
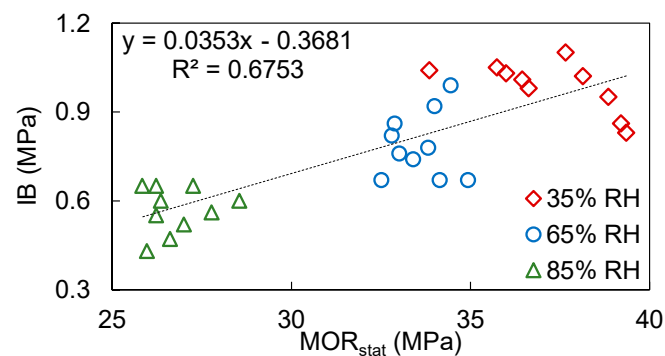

Figure 3. Linear relationship between MOR_{stat} and internal bond (IB) strength of the Medite Tricoya® MDF samples conditioned at three different humidity.
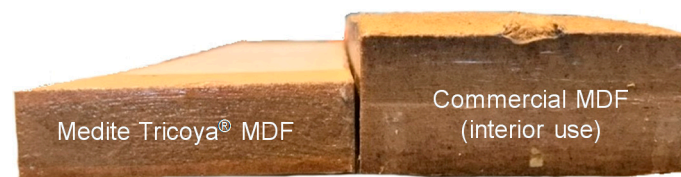

Figure 4. Medite Tricoya® and commercial standard MDF (for interior use) samples after accelerated aging test. Note the double thickness in the commercial MDF sample.

Acoustic resonance measurements were used to determine the MOE_{dyn} (Figure 5). These values represent the mean stiffness, whilst MOE_{stat} represents the local stiffness of the samples at the highly stressed areas of a specific test set-up [50]. MOE_{dyn} was found to differ significantly between // and $\perp$ samples only for the dry condition, i.e., 35% RH. As expected, the increase of RH from dry/standard (35 and 65% RH) to wet (85% RH) conditions resulted in a considerable decrease in MOE_{dyn} in both directions.Resonance frequency of MDF samples decreased with the increase in moisture content and thus affected the MOE_{dyn}. This is because at a dryer state, molecular chains in the amorphous regions of the wood cell wall are distorted with the presence of microvoids between the molecular chains, resulting in lower internal friction, resulting in higher MOE_{dyn}. On the contrary, when moisture content increases, water molecules are embedded in the microvoids and rearrange the distorted molecular chains in the amorphous region. If the moisture content increases further, water acts as a plasticizer and decreases the cohesive forces between molecules, resulting in a higher internal friction and leading to the decrease in MOE_{dyn} [51]. With the increase of RH from 35 to 65%, the average MOE_{dyn} reduction of Medite Tricoya® samples was negligible, i.e., 1%. When the RH was further raised from 65% to 85%, the reduction of MOE_{dyn} was 26%. In addition, MOE_{dyn} values in the perpendicular samples were found lower than the corresponding values in the parallel samples. However, those differences were found to be statistically insignificant. A previous study by Han et al. [26] showed that reduction of stress wave velocity along the perpendicular direction compared to the parallel direction for wood-based panels (plywood, oriented strand board and particleboard) depends on the anisotropic properties

of the products. Smaller differences between the two directions in MDF samples implies a uniform product. However, as expected, MOE_{dyn} values were higher than the static values approximately by 40%. Wood-based panels contain a significant number of glued interfaces, and such a difference is generally explained by the different rates of stresses applied in the dynamic and static tests [52]. The differences between the MOE_{dyn} and MOE_{stat} values were higher at a higher RH. It was 33%, 37% and 49% higher at 35%, 65% and 85% RH conditions, respectively. This is because moisture affects the stress-wave properties for wood-based panels, as they can swell considerably during moisture uptake. The swelling often leads to bond failures and to changes of their internal structure, and as a result, to a decrease of stress wave velocity with the increase in panel moisture content [26].
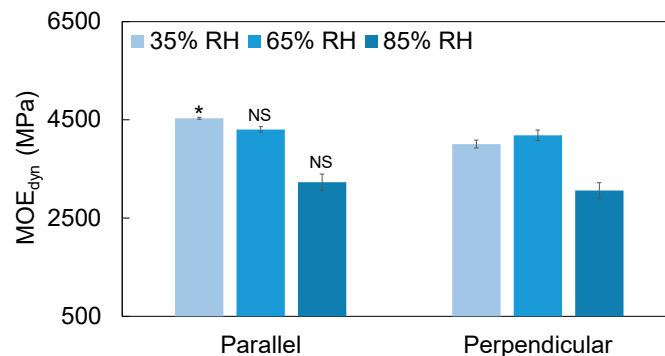

Figure 5. Dynamic modulus of elasticity (MOE_{dyn}) of Medite Tricoya® MDF samples at different relative humidity levels measured by the acoustic resonance method. Error bars represent 95% confidence intervals for the means. * Significant differences between parallel and perpendicular samples as determined by two-sample t-test at the 0.05 level. NS, non-significant.

Acoustic tools have been used quite successfully to predict MOE_{stat} and MOR_{stat} [26,27,53]. Table 5 shows the multiple regression model summary results. Overall, linear and significant relationships ($p < 0.05$) of MOE_{stat} and MOR_{stat} with MOE_{dyn} were observed at different humid conditions. It was noted that R^2 values were slightly higher between MOE_{dyn} and MOE_{stat} than those between MOE_{dyn} and MOR_{stat}.

Table 5. Model summary of regression statistics for MOE_{stat} and MOR_{stat} prediction.

Parameter	MOE_{stat}		MOR_{stat}	
	Parallel	Perpendicular	Parallel	Perpendicular
R^2	0.987	0.969	0.966	0.925
Adjusted R^2	0.970	0.964	0.960	0.913
Standard error	99.484	97.717	1.020	1.175
Intercept	−412.519	883.65	26.822	28.071
RH coefficient	−5.101	−11.624	−0.140	−0.120
MOE_{dyn} coefficient	0.784	0.573	0.004	0.003
F	227.009	187.664	169.889	74.404
Significance F *	0.000	0.000	0.000	0.000

* Significant at the 0.05 level.

The comparison between the experimental and predicted values is shown in Figure 6. The result indicates that the predicted values are very close to the experimental values. F-values for all models (MOE_{stat} and MOR_{stat} in parallel and perpendicular samples) were highly significant at the 0.05 level (Table 5).

Statistical analysis showed that MOE_{dyn} and RH can be used as predictors of MOE_{stat} and MOR_{stat} of MDF samples. The results also indicated that MOE_{stat} and MOR_{stat} have a positive relationship with MOE_{dyn}.
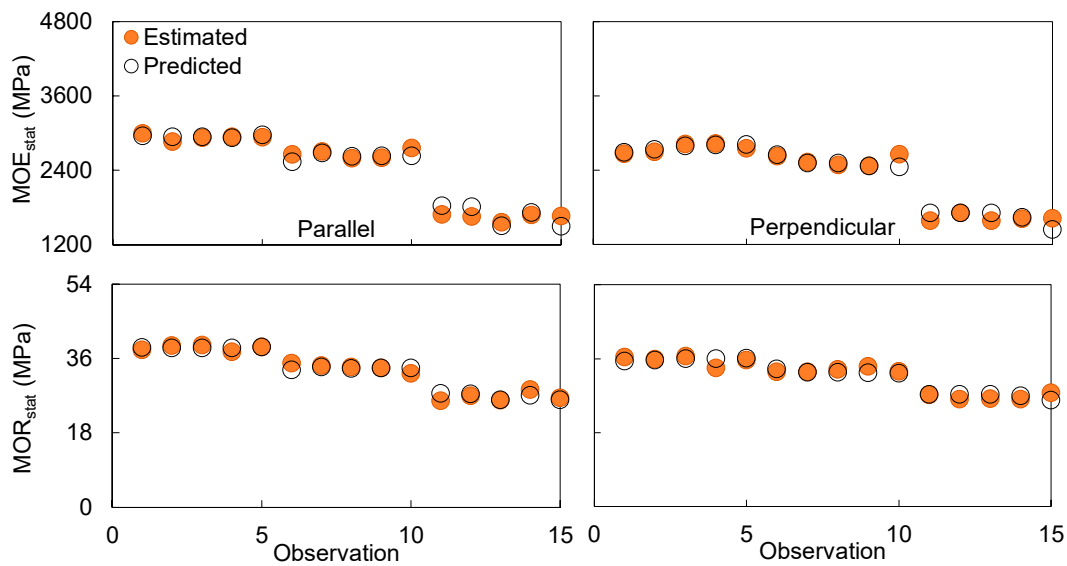
Figure 6. Estimated and predicted values of MOE$_{stat}$ and MOR$_{stat}$ for Medite Tricoya® MDF samples conditioned at three different climatic conditions.

3.3. Finite Element Analysis

Magnitudes of reaction forces and the deflections under these reactions forces in the z-axis direction, as well as values of maximal principal stress for T1, T2 procedures and experimental values, are presented in Table 6. Reaction forces are equal to half of maximal loading force.

Table 6. Magnitudes of displacements, reaction forces, and maximal principal stress for first approach (T1) and second approach (T2) finite element (FE) procedure, and experimental values.

Procedure	Displacement [mm]	Reaction Force [N]	Maximal Principal Stress [MPa]
T1-quasi- static stress /displacement	8.3	599	30.98
T2-extended finite element method	8.9	641	35.60
Experimental value	7.6	563	35.89

Finally, it is necessary to add that the values for the T2 model show the maximal values at the time point when the jump in the damage dissipation energy occurs (Figure 7): thus, in this particular case, at the time increment 0.4623 of 1 with index number 30. At this time, the increment of the crack growth is initiated and the crack propagates [28], i.e., we are at beginning of a fracture mechanism.

The crack occurrence is visualized in Figure 8 using the PHILSM function, i.e., a singled distance function that describes the crack surface [28].

When we compare results obtained from the two computational models using different simulations techniques T1 (quasi-static stress/displacement) and T2 (extended finite element) with the experimental values, we see percental errors of 8.6% and 14.3%. As expected, these percent errors are relatively high. This demonstrates that the used computational methods do not provide reliable results, and thus, can be considered to have a low fidelity. Despite this fact, these techniques are today used as the main techniques in standard design procedures because they are highly efficient [29,31]. To be sure, the errors can be minimized by optimizing the input parameters that imitate the real nature of the studied MDF material; however, that requires more necessary testing, like, for example, creep testing and fracture testing, to obtain those data. This means spending more time to set up experiments, more wasted material for creating samples, as well as time to collect and analyze data sets.
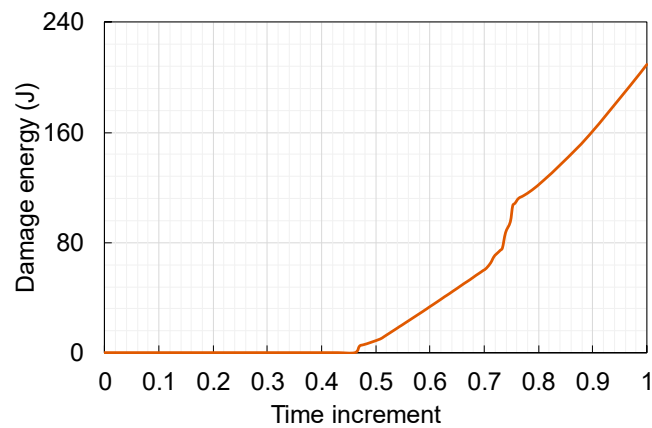
Figure 7. Damage dissipation energy for the extended finite element method model (T2).
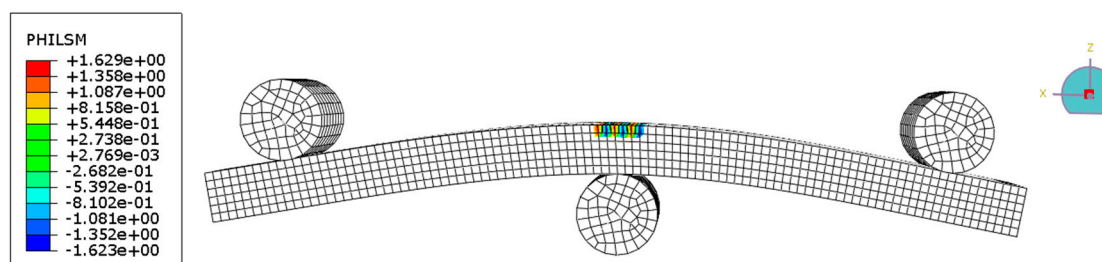

Figure 8. Singled distance function (PHILSM) for T2 model.

A better solution here is to use the help of micromechanical modelling approaches to specify material behaviour on a constituent level that is summarized in [32,54,55], and that will provide more reliable results compared with experimental ones and reduce the need for new sets of tests. More precisely, the employment of concurrent material and structural design applying multiscale models comes in since viscoelastic creep damage models and rheological behavior of MDF material are considered [56]. Here, we mean the time-dependent mechanical repose of MDF on a constant load considering the influence material´s density as well as fiber orientation, and the existence of voids and interfaces in the material microstructure. More importantly, the macroscale computational techniques used in this work do not take into consideration the very significant dependence of mechanical properties on the moisture and temperature. This, as demonstrated in this work, should be included in the computations to precisely predict mechanical material characteristics such as strength, toughness and elasticity as well as to predict the damage mechanism of the panel product.

4. Conclusions

The results obtained in this study showed that, due to the lower hygroscopicity of Medite Tricoya® samples, they absorbed less moisture and became more dimensionally stable even at the highest humidity condition. This MDF type can also retain its IB strength after an accelerated aging test. However, IB strength, MOE_{stat} and MOR_{stat} were reduced from dry to humid conditions. At the highest humid condition (85% RH), strength and stiffness values did not differ significantly between parallel and perpendicular samples. In addition, multiple regression models were developed from MOE_{dyn} and RH to predict the strength and stiffness of Medite Tricoya® MDF. In both parallel and perpendicular directions, highly significant relationships were observed. Developed models could predict the MOE_{stat} and MOR_{stat} values of Medite Tricoya® MDF samples at any humid conditions, which produced an excellent fit to the measured values. This experimental outcome could ensure reliable and safe predictions of Medite's Tricoya® MDF strength and stiffness properties for intended end uses.

This study also showed that employing macroscale computational modelling approaches that are nowadays broadly used in engineering practice, such as quasi-static stress/displacement (T1) and extended finite element (T2) techniques, are not sufficient to obtain reliable results for MDF. These modelling methods are highly efficient and fast, but low in fidelity. Therefore, in future work, it is necessary to employ more precise multiscale models to secure more efficient material and structure design approaches. Additionally, multiscale models will reduce the necessity to set up new testing whenever we need to change the components proportion or component material in composite material.

References

1. Bianchi, S.; Thömen, H.; Junginger, S.; Pichelin, F. Medium density boards made of groundwood fibres: An analysis of their mechanical and physical properties. *Eur. J. Wood Wood Prod.* **2018**, *77*, 71–77. [CrossRef]

2. Ayrilmis, N.; Winandy, J.E. Effects of Post Heat-Treatment on Surface Characteristics and Adhesive Bonding Performance of Medium Density Fiberboard. *Mater. Manuf. Process.* **2009**, *24*, 594–599. [CrossRef]

3. Palardy, R.D.; Haataja, B.A.; Shaler, S.M.; Williams, A.D.; Laufenberg, T.L. Pressing of wood composite panels at moderate temperature and high moisture content. *For. Prod. J.* **1989**, *39*, 27–32.

4. Li, X.; Li, Y.; Zhong, Z.; Wang, D.; Ratto, J.A.; Sheng, K.; Sun, X.S. Mechanical and water soaking properties of medium density fiberboard with wood fiber and soybean protein adhesive. *Bioresour. Technol.* **2009**, *100*, 3556–3562. [CrossRef] [PubMed]

5. Mohebby, B.; Gorbani-Kokandeh, M.; Soltani, M. Springback in acetylated wood based composites. *Constr. Build. Mater.* **2009**, *23*, 3103–3106. [CrossRef]

6. Findley, W.N.; Lai, J.S.; Onaran, K. *Creep and Relaxation of Nonlinear Viscoelastic Materials*; North-Holland Publishing Company: New York, NY, USA, 1976.

7. Ji, X.; Li, B.; Yuan, B.; Guo, M. Preparation and characterizations of a chitosan-based medium-density fiberboard adhesive with high bonding strength and water resistance. *Carbohydr. Polym.* **2017**, *176*, 273–280. [CrossRef] [PubMed]

8. Gao, S.; Liu, Y.; Wang, C.; Chu, F.; Xu, F.; Zhang, D. Synthesis of Lignin-Based Polyacid Catalyst and Its Utilization to Improve Water Resistance of Urea-formaldehyde Resins. *Polymers* **2020**, *12*, 175. [CrossRef]

9. Mamiński, M.Ł.; Trzepałka, A.; Auriga, R.; H'Ng, P.S.; Chin, K.L. Physical and mechanical properties of thin high density fiberboard bonded with 1,3-dimethylol-4,5-dihydroxyethyleneurea (DMDHEU). *J. Adhes.* **2020**, *96*, 679–690. [CrossRef]

10. Oliveira, S.L.; Freire, T.P.; Mendes, R.F. The Effect of Post-Heat Treatment in MDF Panels. *Mater. Res.* **2017**, *20*, 183–190. [CrossRef]

11. Garcia, R.A.; Cloutier, A.; Riedl, B. Dimensional stability of MDF panels produced from heat-treated fibres. *Holzforschung* **2006**, *60*, 278–284. [CrossRef]

12. Lee, T.C.; Mohd Pu'ad, N.A.S.; Selimin, M.A.; Manap, N.; Abdullah, H.Z.; Idris, M.I. An overview on development of environmental friendly medium density fibreboard. *Mater. Today Proc.* **2020**, *29*, 52–57. [CrossRef]

13. Dazmiri, M.K.; Kiamahalleh, M.V.; Kaiamahalleh, M.V.; Mansouri, H.R.; Moazami, V. Revealing the impacts of recycled urea-formaldehyde wastes on the physical-mechanical properties of MDF. *Eur. J. Wood Wood Prod.* **2018**, *77*, 293–299. [CrossRef]

14. Papadopoulos, A.N.; Gkaraveli, A. Dimensional stabilization and strength of particleboard by chemical modification with propionic anhydride. *Holz Roh Werkst.* **2003**, *61*, 142–144. [CrossRef]

15. Kajita, H.; Imamura, Y. Improvement of physical and biological properties of particleboards by impregnation with phenolic resin. *Wood Sci. Technol.* **1991**, *26*, 63–70. [CrossRef]

16. Nasir, M.; Gupta, A.; Beg, M.D.H.; Chua, G.K.; Asim, M. Laccase application in medium density fibreboard to prepare a bio-composite. *RSC Adv.* **2014**, *4*, 11520–11527. [CrossRef]

17. Rowell, R.M.; Youngquist, J.A.; Rowell, J.S.; Hyatt, J.A. Dimensional stability of aspen fiberboard made from acetylated fiber. *Wood Fiber Sci.* **1991**, *23*, 558–566.

18. Mai, C.; Direske, M.; Varel, D.; Weber, A. Light medium-density fibreboards (MDFs): Does acetylation improve the physico-mechanical properties? *Eur. J. Wood Wood Prod.* **2016**, *75*, 739–745. [CrossRef]

19. Gomez-Bueso, J.; Westin, M.; Torgilsson, R.; Olesen, P.O.; Simonson, R. Composites made from acetylated lignocellulosic fibers of different origin—Part I. Properties of dry-formed fiberboards. *Holz Roh Werkst.* **2000**, *58*, 9–14. [CrossRef]

20. Mahlberg, R.; Paajanen, L.; Nurmi, A.; Kivisto, A.; Koskela, K.; Rowell, R.M. Effect of chemical modification of wood on the mechanical and adhesion properties of wood fiber/polypropylene fiber and polypropylene/veneer composites. *Eur. J. Wood Wood Prod.* **2001**, *59*, 319–326. [CrossRef]

21. Vick, C.B.; Krzysik, A.; Wood, J.E., Jr. Acetylated, isocyanate-bonded flakeboards after accelerated aging: Dimensional stability and mechanical properties. *Holz Roh Werkst.* **1991**, *49*, 221–228. [CrossRef]

22. Korai, H. Effects of low bondability of acetylated fibers on mechanical properties and dimensional stability of fiberboard. *J. Wood Sci.* **2001**, *47*, 430–436. [CrossRef]

23. Ghorbani, M.; Bavaneghi, F. Effect of Press Cycle Time on Application Behavior of Board Made from Chemically Modified Particles. *Drv. Ind.* **2016**, *67*, 25–31. [CrossRef]

24. Legg, M.; Bradley, S. Measurement of stiffness of standing trees and felled logs using acoustics: A review. *J. Acoust. Soc. Am.* **2016**, *139*, 588–604. [CrossRef]

25. Wang, X. Acoustic measurements on trees and logs: A review and analysis. *Wood Sci. Technol.* **2013**, *47*, 965–975. [CrossRef]

26. Han, G.; Wu, Q.; Wang, X. Stress-wave velocity of wood-based panels: Effect of moisture, product type, and material direction. *For. Prod. J.* **2006**, *56*, 28–33.

27. Guan, C.; Guan, C.; Zhou, L.; Wang, X. Dynamic determination of modulus of elasticity of full-size wood composite panels using a vibration method. *Constr. Build. Mater.* **2015**, *100*, 201–206. [CrossRef]

28. Dassault Systèmes. *SIMULIA User Assistance/Analysis Procedure*; Dassault Systèmes: Vélizy-Villacoublay, France, 2019.

29. Belytschko, T.; Black, T. Elastic crack growth in finite elements with minimal remeshing. *Int. J. Numer. Methods Eng.* **1999**, *45*, 601–620. [CrossRef]

30. Barbero, E. *Finite Element Analysis of Composite Materials Using Abaqus™*; CRC Press: Boca Raton, FL, USA, 2013; p. 444.

31. Barbero, E. *Introduction to Composite Materials Design*, 3rd ed.; CRC Press: Boca Raton, FL, USA, 2017; p. 534.

32. Aboudi, J.; Arnold, S.M.; Bednarcyk, B.A. *Micromechanics of Composite Materials: A Generalized Multiscale Analysis Approach*, 1st ed.; Butterworth-Heinemann Ltd.: Oxford, UK, 2013.

33. European Committee for Standardization. *Wood-Based Panels—Determination of Moisture Content*; EN 322; European Committee for Standardization: Brussels, Belgium, 1993.

34. European Committee for Standardization. *Wood-Based Panels—Determination of Density*; EN 323; European Committee for Standardization: Brussels, Belgium, 1993.

35. European Committee for Standardization. *Wood-Based Panels—Determination of Dimensional Changes Associated with Changes in Relative Humidity*; EN 318; European Committee for Standardization: Brussels, Belgium, 2002.

36. European Committee for Standardization. *Particleboards and Fiberboards—Determination of Swelling in Thickness after Immersion in Water*; EN 317; European Committee for Standardization: Brussels, Belgium, 1993.

37. European Committee for Standardization. *Particleboards and Fibreboards—Determination of Tensile Strength Perpendicular to the Plane of the Board*; EN 319; European Committee for Standardization: Brussels, Belgium, 1993.

38. European Committee for Standardization. *Wood-Based Panels—Determination of Modulus of Elasticity in Bending and of Bending Strength*; EN 310; European Committee for Standardization: Brussels, Belgium, 1993.

39. Ahmed, S.A.; Adamopoulos, S. Acoustic properties of modified wood under different humid conditions and their relevance for musical instruments. *Appl. Acoust.* **2018**, *140*, 92–99. [CrossRef]

40. Rowell, R.M.; Ibach, R.E.; McSweeny, J.; Nilsson, T. Understanding decay resistance, dimensional stability and strength changes in heat-treated and acetylated wood. *Wood Mater. Sci. Eng.* **2009**, *4*, 14–22. [CrossRef]

41. Ayrilmis, N. Effect of panel density on dimensional stability of medium and high density fiberboards. *J. Mater. Sci.* **2007**, *42*, 8551–8557. [CrossRef]

42. Ganev, S. Modeling of the Hygromechanical Warping of Medium Density Fiberboard. Ph.D. Thesis, Forestry Faculty, University of Laval, Québec, QC, Canada, 2002.

43. Bekhta, P.; Niemz, P. Effect of relative humidity on some physical and mechanical properties of different types of fibreboard. *Eur. J. Wood Wood Prod.* **2009**, *67*, 339–342. [CrossRef]

44. Pritchard, J.; Ansell, M.P.; Thompson, R.J.H.; Bonfield, P.W. Effect of two relative humidity environments on the performance properties of MDF, OSB and chipboard. *Wood Sci. Technol.* **2001**, *35*, 395–403. [CrossRef]

45. McNatt, J.D.; Wellwood, R.W.; Bach, L. Relationships between small-specimen and large panel bending tests on structural wood-based panels. *For. Prod. J.* **1990**, *40*, 10–16.

46. Wu, Q.; Suchsland, O. Effect of moisture on the flexural properties of commercial oriented strandboards. *Wood Fiber Sci.* **1997**, *29*, 47–57.

47. Halligan, A.F.; Schniewind, P. Prediction of particleboard mechanical properties at various moisture contents. *Wood Sci. Technol.* **1974**, *8*, 68–78.

48. Feist, W.C.; Rowell, R.M.; Ellis, W.D. Moisture sorption and accelerated weathering of acetylated and methacrylated aspen. *Wood Fiber Sci.* **1991**, *23*, 128–136.

49. Kojima, Y.; Suzuki, S. Evaluating the durability of wood-based panels using internal bond strength results from accelerated aging treatments. *J. Wood Sci.* **2011**, *57*, 7–13. [CrossRef]

50. Nocetti, M.; Brancheriau, L.; Bacher, M.; Brunetti, M.; Crivellaro, A. Relationship between local and global modulus of elasticity in bending and its consequence on structural timber grading. *Eur. J. Wood Wood Prod.* **2013**, *71*, 297–308. [CrossRef]

51. Akitsu, H.; Norimoto, M.; Morooka, T.; Rowell, R.M. Effect of humidity on vibrational properties of chemically modified wood. *Wood Fiber Sci.* **1993**, *25*, 250–260.

52. Bos, F.; Casagrande, S. On-line non-destructive evaluation and control of wood-based panels by vibration analysis. *J. Sound Vib.* **2003**, *268*, 403–412. [CrossRef]

53. Guan, C.; Liu, J.; Zhang, H.; Wang, X.; Zhou, L. Evaluation of modulus of elasticity and modulus of rupture of full-size wood composite panels supported on two nodal-lines using a vibration technique. *Constr. Build. Mater.* **2019**, *218*, 64–72. [CrossRef]

54. Souza, F.V.; Castro, L.S.; Camara, S.L.; Allen, D.H. Finite-element modeling of damage evolution in heterogeneous viscoelastic composites with evolving cracks by using a two-way coupled multiscale model. *Mech. Compos. Mater.* **2011**, *47*, 95–108. [CrossRef]

55. Šliseris, J.; Andrä, H.; Kabel, M.; Dix, B.; Plinke, B.; Wirjadi, O.; Frolovs, G. Numerical prediction of the stiffness and strength of medium density fiberboards. *Mech. Mater.* **2014**, *79*, 73–84. [CrossRef]

56. Huč, S.; Hozjan, T.; Svensson, S. Rheological behavior of wood in stress relaxation under compression. *Wood Sci. Technol.* **2018**, *52*, 793–808. [CrossRef]